JOURNAL OF GEOPHYSICAL RESEARCH, VOL. 105, NO. D1, PAGES 1337-1349, JANUARY 20, 2000

Latitudinal variations of trace gas concentrations in the free troposphere measured by solar absorption spectroscopy during a ship cruise

J. Notholt,[1] G.C. Toon,[2] C.P. Rinsland,[3] N.S. Pougatchev,[4]
N.B. Jones,[5] B.J. Connor,[5] R. Weller,[6] M. Gautrois,[7] and O. Schrems [6]

Abstract. The latitudinal variations of atmospheric trace gas column abundances have been measured during a ship cruise between 57°N and 45°S on the central Atlantic. The measurements were performed in October 1996 using high-resolution solar absorption spectroscopy in the infrared. The analysis method employed permits the retrieval of the total column densities of 20 different trace gases and for a few compounds the vertical mixing ratio profiles. For CH_4 an interhemispheric difference of 3% was observed. The total columns of the shorter-lived trace gases CO and C_2H_6, analyzed between 57°N and 45°S, reveal a slight maximum in the tropics and a substantial increase north of 45°N. The total columns of C_2H_2 and HCN, detectable between 30°N and 30°S, reveal a maximum in the tropics of the Southern Hemisphere. For CH_2O, studied between 57°N and 45°S, a well-pronounced maximum is observed in the tropics. The profile retrieval gives high mixing ratios for CO, C_2H_6, and O_3 north of 40°N in the lower troposphere. In the tropics high concentrations are found for all three compounds in the entire troposphere, even above 12 km. The measurements have been used to estimate averaged mixing ratios of the trace gases for the free troposphere between 0 and 12 km. In the tropics the data give high values: for example, more than 200 pptv for HCN, 750 pptv for CH_2O, 100 ppbv for CO and 100 pptv for C_2H_2. These values are comparable to or higher than what has been observed at midlatitudes, indicating the importance of biomass burning emissions on the tropospheric composition.

1. Introduction

Measurements of the latitudinal variations of trace gases are of great importance for understanding the chemical and dynamical processes that control the distributions of these gases in the free troposphere and stratosphere. Observations are especially needed to understand the global impact of anthropogenic pollution in the Northern Hemisphere and biomass burning in the tropical Southern Hemisphere [*Graedel and Crutzen*, 1993; *Levine*, 1996]. Since trace gases enter the stratosphere primarily in the tropics, this region has an especially important influence on stratospheric composition.

Ground-based in situ measurements can yield time series of local atmospheric trace gas concentrations [e.g., *World Metereological Organization (WMO)*, 1997]. On the other hand, satellite observations provide atmospheric trace gas concentrations above typically 15 km on a global scale [e.g., *Russell et al.*, 1993; *Gunson et al.*, 1996]. However, only a few data exist for the remote free troposphere. The tropical regions have been studied during the Southern Tropical Atlantic Region Experiment (STARE), [see *Andreae et al.*, 1996] and Pacific Exploratory Mission (PEM) [e.g. *Hoell et al.*, 1996, *Hoell et al.*, 1997]. Observations at midlatitudes are described by *Angeletti and Restelli* [1994].

Spectroscopic remote observations from the surface with the Sun as light source sample trace gas concentrations of up to 30 different trace gases in the whole atmosphere, including the free troposphere [e.g., *Rao and Weber*, 1992]. In addition, for the altitude range where the pressure broadening of the spectral lines can be resolved, an analysis can yield concentration profiles for a few atmospheric layers.

In October-November 1996 we participated in a ship cruise across the Atlantic on board the German research vessel *Polarstern* to perform high-resolution solar absorption measurements in the infrared by Fourier transform infrared (FTIR) spectroscopy. From these observations, the concentrations of up to 20 different atmospheric trace gases between approximately 57°N and 45°S latitude were determined. The aim of the FTIR measurements was to study the latitudinal variations of atmospheric trace gases in the free troposphere and the impact of anthropogenic emissions and the tropical biomass burning from the continents on the central Atlantic.

[1]Alfred Wegener Institute for Polar and Marine Research, Potsdam, Germany.
[2]Jet Propulsion Laboratory, California Institute of Technology, Pasadena.
[3]Atmospheric Sciences Division, NASA Langley Research Center, Hampton, Virginia.
[4]Christopher Newport University, Physics Department, Newport News, Virginia.
[5]National Institute of Water and Atmospheric Research, Lauder, New Zealand.
[6]Alfred Wegener Institute for Polar and Marine Research, Bremerhaven, Germany.
[7]Institute for Atmospheric Chemistry, Forschungszentrum Jülich, Jülich, Germany.

Paper number 1999JD900940.
0148-0227/00/1999JD900940$09.00

2. Experimental Methods

The experiments have been performed using a Bruker 120M interferometer. The instrument was installed in a thermostated laboratory container on the helicopter deck in the back of the ship, 10 m above sea level. The solar tracker was mounted on the container's roof. It was driven, under control of a quadrant diode, to follow the Sun despite all ship movements. In order to overcome the ship movements, the solar tracker was modified to move much faster than for ground-based observations. To reduce the influence of ship rolling (ship movements perpendicular to the direction of the ship), the scanning arm of the interferometer had been installed parallel to the ship's body. However, later on it was found that pitching of the ship (up and down movements of the forepart of the deck and quarter-deck) has a stronger influence than rolling, because the rolling was sufficiently reduced by the stabilizer fins of the ship. Unfortunately, it was not possible to rotate the instrument.

For wind velocities of about 15 m/s, the interferometer and the solar tracker worked satisfactorily. Under stronger wind conditions the motors of the solar tracker could no longer keep the image of the Sun on the entrance aperture. Furthermore, for such wind velocities the recording of spectra yielded erroneous interferograms, because the scanning mirror had to drive "up and down" following pitching. However, under these weather conditions the measurements had to be stopped anyway because the sea spray splashed against the mirrors of the solar tracker.

The strongest disturbances on the interferometer were assumed to be due to the vibrations of the ship engines in a frequency range of 20–30 Hz. The stability of the interferometer has been tested by studying the variability of the center burst intensity during the alignment mode, using an artificial light source. The intensity in the IR was found to vary by 1–2%, similar to our observations in Spitsbergen. However, in the UV (at 300 nm) the peak-to-peak intensity fluctuations increased up to 30%, preventing any measurements. Furthermore, the alignment of the interferometer was checked daily by studying the interference fringes using an external HeNe-laser equipped with a 8 cm diameter telescope to cover the whole beam area. After the installation the alignment was found to be stable during the whole cruise. Under normal weather condidtions (wind speeds less than 15 m/s) the fringes did not visibly change as a function of the ships movements or motor vibrations.

Spectra were recorded between 750 and 6000 cm^{-1} with an optical path difference (OPD) of 200 cm, corresponding to an unapodized resolution of 0.005 cm^{-1}, using the Sun as the light source. Typically, groups of two to six consecutive single spectra were averaged, yielding measurement times up to 20 min. In order to increase the signal-to-noise ratio (S/N), interference filters have been used to narrow the optical bandwidth. To get a good latitudinal coverage, each spectral region was recorded in the morning, around noon, and in the evening. Owing to the use of the band limit interference filters, not all trace gases could be studied on each day.

The fact that the humidity is high in the tropics, especially at sea level, restricts the number of molecules which can be analyzed in the IR, due to interfering water vapor absorptions. Compared to our observations in Spitsbergen (79°N) all trace gases detected there [see *Notholt et al.*, 1997a, Table 1] could be measured during the cruise, except NO. For this molecule, strong interference from nearby water lines prevented the analysis in the tropics, even at noon for solar zenith angles (SZAs) around 0°.

In a remote area like the middle of the Atlantic, the influence of the ship's exhaust gases on the spectroscopic results has to be checked. Any measurement directly through the exhaust plume was always avioded. However, such situations occurred only on a few days around noon. Under those circumstances the ship's route was changed by around 45° for 1 hour, allowing the recording of a set of spectra without disturbances from the exhaust plume. Overall, the exhaust plume was found to have a negligible influence on the results.

3. Data Analysis

The microwindows used to analyze the trace gases, together with the interfering gases which have been fitted, are given in Table 1. The spectroscopic parameters have been taken from the 1996 HITRAN [*Rothman et al.*, 1998] and Atmospheric Trace Molecule Spectroscopy Experiment (ATMOS) database [*Brown et al.*, 1996]. Spectral parameters for C_2H_6 were based on the measurements of *Pine and Stone* [1996]. The updated parameters for C_2H_6 have been described by *Rinsland et al.* [1998a].

The total column densities and the vertical concentration profiles have been determined using two different line-by-line least squares algorithms, SFIT2 and GFIT. Both algorithms are described in the literature and will not be discussed here in detail.

SFIT2 [*Pougatchev et al.*, 1995; *Rinsland et al.*, 1998a] has been developed as a profile retrieval algorithm. It is based on the semiempirical approach to the optimal estimation method [*Rodgers et al.*, 1976]. The analysis is performed by fitting one or more windows simultaneously with the profile of one or two molecules retrieved in 29 atmospheric layers. Additionally, the a priori profiles of one or more molecules can be scaled by multiplicative factors to account for interferences. For the interpretation of the data the results of the individual layers are summed up to a few thick layers, for example, 0–4 km, 4–12

Table 1. Microwindows Used in the Analysis Together With the Interfering Trace Gases Fitted

Molecule	Spectral Regions	Interfering Gases
CH_4	2601.71–2604.15	N_2O
	2903.55–2904.25	H_2O, HCl, O_3, HDO
	4277.61–4278.01	H_2O, HDO
N_2O	2441.8–2444.4	CO_2
	2481.20–2482.50	
	2806.05–2806.55	
CFC-12	920.09–923.89	H_2O, CO_2
	1160.13–1162.03	HDO, O_3, N_2O, H_2O
CFC-22	828.80–829.25	O_3, H_2O
CO	2057.70–2057.90	H_2O, N_2O, O_3
	2069.55–2069.80	H_2O, N_2O, O_3
	2157.30–2159.35	H_2O, N_2O, O_3
C_2H_6	2967.60–2967.94	H_2O, CH_4, O_3
C_2H_2	3250.43–3250.74	H_2O
CH_2O	2869.44–2870.33	CH_4, O_3, NO_2, HDO
HCN	3287.10–3287.50	H_2O
	3299.42–3299.64	H_2O
	3305.35–3305.60	H_2O
COS	2051.15–2055.95	O_3, CO
O_3	1002.58–1003.50	H_2O
	1003.90–1004.38	H_2O
	1004.58–1005.00	H_2O
H_2O	2870.00–2873.30	CH_4
	3019.75–3019.95	
HDO	2611.50–2613.28	CO_2
	2640.40–2643.14	CH_4, CO_2

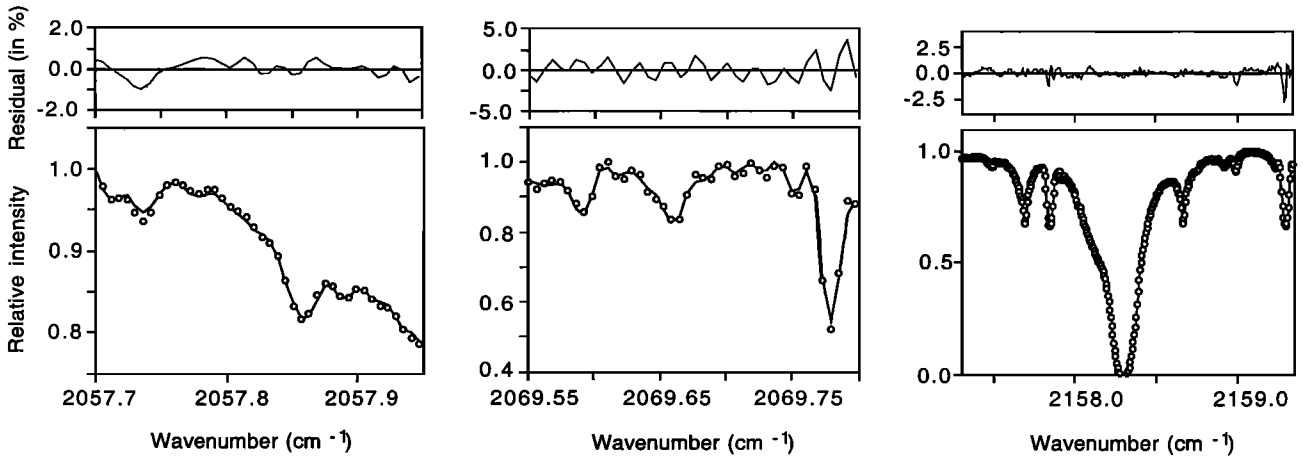

Figure 1. Example of a fit to a spectrum, measured at 31°N at a resolution of 0.0055 cm^{-1}. All three regions have been fitted simultaneously using SFIT2 to retrieve the volume mixing ratio (vmr) profile of CO.

km, and above 12 km, which provide partial columns that are nearly independent, as indicated by averaging kernel calculations. Figure 1 gives an example of the fits for the three spectral regions covering CO, which have been analyzed simultaneously using SFIT2.

Averaging kernels provide the theoretical basis for determining the altitude sensitivity of a given atmospheric measurement (see, for example, *Rodgers* [1990] and *Connor et al.* [1995]). Figure 2 presents averaging kernels calculated for the cruise observations of CO, C_2H_6, and O_3. They have been calculated with as many suitable spectral lines as possible with different optical depths in order to combine the effects of different altitude sensitivities (three for CO and O_3, one for C_2H_6, see Table 1). An attempt was made to use spectroscopic data from other spectral regions, for example, O_3 lines at 3040 cm^{-1}. However, since these lines do not belong to the same band pass as the ones around 1000 cm^{-1}, a simultaneous fit of all microwindows from different band passes failed in many cases, probably because of temporal or spatial variations in the atmospheric composition.

The altitude borders have been chosen in a way that the averaging kernels show good sensitivity in the respective altitude regions and fairly good discrimination outside them. For CO, partial columns have been retrieved for three layers, 0–4, 4–12, and above 12 km. The profile for C_2H_6 could only be retrieved in two atmospheric layers, 0–12 and above 12 km. For O_3 the analysis was performed for the altitudes 0–12, 12–20, and above 20 km. As can be seen, all averaging kernels overlap to some degree indicating that the results retrieved for each layer are to some extent influenced by the other layers. This must be considered in the interpretation.

Originally, GFIT was developed for the retrieval of total column densities [e.g., *Toon et al.*, 1992; *Notholt et al.*, 1997a]. The program has been further adapted to retrieve the partial columns in a few atmospheric layers as will be explained in a forthcoming paper. Unlike SFIT2 the modified version of GFIT uses no constraints on the profiles during the analysis; the different altitude regions are treated as independent.

During the cruise, balloon sondes were launched daily from the *Polarstern*, yielding the pressure–temperature (pT) and ozone profiles up to 30 km together with the profiles of the relative humidity up to about 10 km. The relative humidity data served as inputs for the forward models. The initial volume mixing ratio (vmr) profiles of CO and C_2H_6 are based on observations by *Talbot et al.* [1996] measured during the Transport and Atmospheric Chemistry Near the Equator–Atlantic (TRACE A) campaign in September–October 1992 above the Atlantic. For CO, two different profiles have been used, one for the northern and another for the southern Atlantic. The initial vmr profiles for all other trace gases, including O_3, were taken from balloon flights, launched at 34°N [*Peterson and Margitan*, 1995]. As discussed later, the data of the ozone sondes, launched daily during the cruise, have only been used for comparison with the retrieved profiles.

Prior to the analysis the balloon profiles were transformed vertically above the tropopause by a streching parameter degree of subsidence (DOS), as explained in detail by *Toon et al.*, [1992] and *Notholt et al.*, [1997a]. This transformation of the initial vmr–profiles accounts for vertical motions in the stratosphere, like the difference in the tropopause height or the subsidence caused by diabatic cooling during meridional transport.

4. Error Discussion

In the following we will not give a complete error discussion, but refer only to the main sources of error, which have to be considered in the interpretation of our data. A detailed error discussion of similar FTIR observations, performed by using a Bruker model 120 M interferometer and the SFIT2 or GFIT analysis are given by *Rinsland et al.* [1998a] and *Toon et al.* [1992].

The uncertainties caused by the limited S/N of the spectra and interfering spectral lines are given for all molecules in Table 2. Typical values have been given for single spectra and for daily averages. Since the temperature profiles have been measured daily by balloon sondes, the error introduced in the total columns retrieved is estimated to be about 1%. The influence of the uncertainties in the vmr profile on the total columns is estimated to be less than 5%. The consistency of the forward models and the retrieval programs can be checked by comparing the total columns derived by SFIT2 with the results derived by GFIT. The total columns retrieved differ by up to 5%, in agreement with the "'spectral fitting algorithm

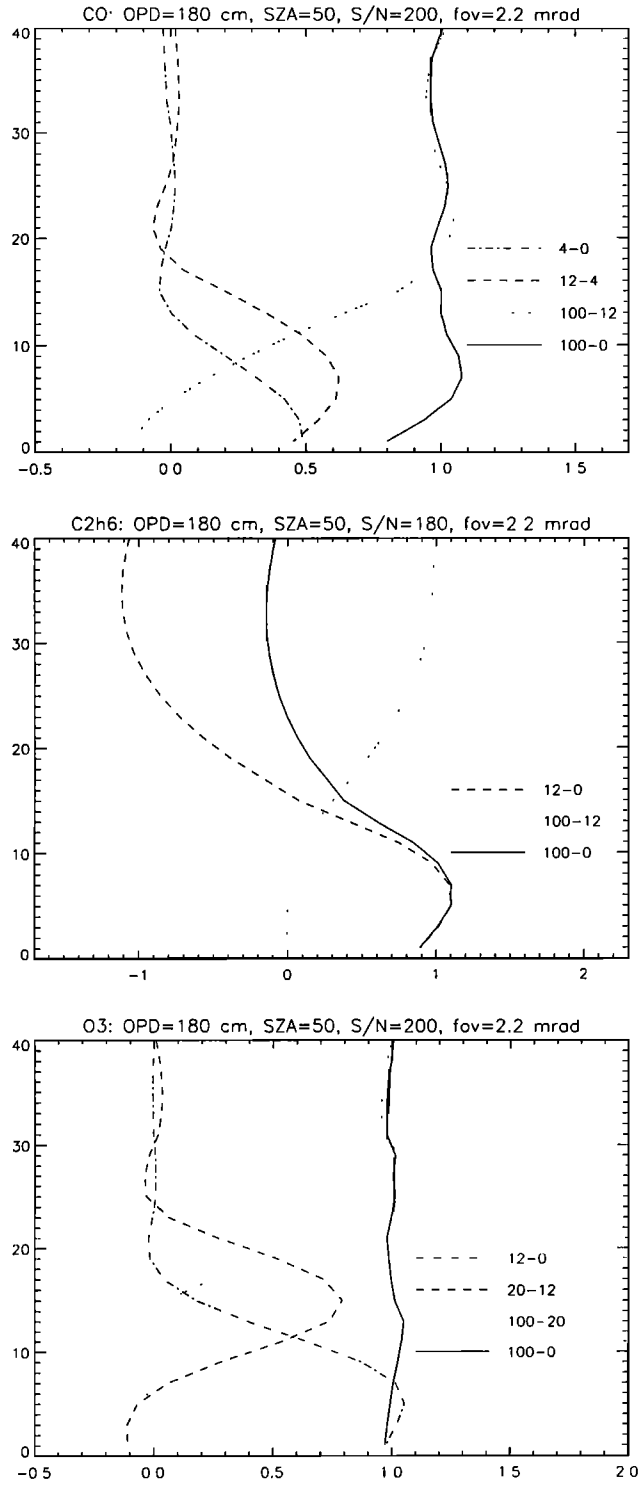

Figure 2. Averaging kernels for CO, C2H6 and O3. They have been calculated for the optical path difference (OPD), the field of view (fov), the solar zenith angle (SZA) and the signal to noise ratio (S/N), as given on the top of the panels.

intercomparison campaign" performed within the Network of Detection of Stratospheric Change (NDSC) [*Zander et al.*, 1993].

The uncertanties in the profile retrieval are much more difficult to quantify. The main sources of error are the following:

1. One source of error is the vertical profile shape. As already mentioned, averaging kernels quantify the theoretical sensitivity of the retrieval for each layer and the overlap of kernels for different layers. Averaging kernel calculations guided our selections of the altitude regions we combined to calculate the partial columns.

2. There is a second source of error in the assumptions on the initial guess profile and limited S/N. Since the atmospheric vmr profiles are not known, the influence of the initial profiles on the partial columns is difficult to quantify. For low S/N ratios the results will be shifted toward the initial guess profiles. To test the influence of the initial guess profiles on the partial columns we have analyzed the spectra using different initial profiles taken from the literature [e.g., *Talbot et al.*, 1996; *Peterson and Margitan*, 1995]. The results differed by 10–20%, with the higher values for CO and C_2H_6 in the upper atmospheric layer and for O_3 in the lowest layer. However, the latitudinal shape of the partial columns was influenced only to a minor extent.

3. A third source of error is the instrumental line shape function. The instrument function influences the retrieved profile to a great extent. During the cruise we checked the alignment and stability of the interferometer daily by illuminating the whole beam area and studying the interference fringes in the visible, as discussed above. Furthermore, profile retrievals of CO_2, known to have a virtually constant vmr profile, give a good indication of the correctness of the instrumental line shape.

The comparison with the other correlative data sets allowed us to test the accuracy of the profile retrieval. In particular, the comparison with the O_3 ballon data (Figures 7a–7c) gives a good indication of the accuracy of the profile retrieval. As can be seen, the partial columns retrieved differ on the average by 10%, in agreement with the errors discussed above.

Furthermore, comparisons were made of the results retrieved using SFIT2 with corresponding results using GFIT. The partial columns retrieved by both methods differed by up to 20%. Most of this error is artificially introduced due to the fundamental difference in the methodology of forming the partial columns. SFIT2 smoothly adjusts the entire a priori profile, while GFIT treats the summed layers as different surrogate gases. Thus agreement at this level for a profile retrieval is acceptable and lies within the errors discussed.

Table 2. Typical Values for the Uncertainties of the Total Columns Retrieved Caused by the S/N (1σ) and the Uncertainties of the Line Parameters

Species	Single Spectrum Uncertainty, %	Daily Averaged Uncertainty, %	Line Parameter Uncertainty, %
CFC–12	1.6	0.7	10.0
CFC–22	50.0	12.0	10.0
CO	5.0	1.5	5.0
C_2H_6	15.0	3.0	10.0
C_2H_2	100.0	20.0	10.0
CH_2O	10.0	3.0	10.0
HCN	15.0	5.0	10.0
COS	25.0	10.0	5.0
O_3	2.0	0.5	5 0
H_2O	1.5	0.7	3.0
HDO	1.3	0.5	3.0

The second column from the left gives the 1σ uncertainties for a single spectrum and the third column gives them for daily averages. The right column gives the uncertainties attributed to errors in the assumed spectral line parameters.

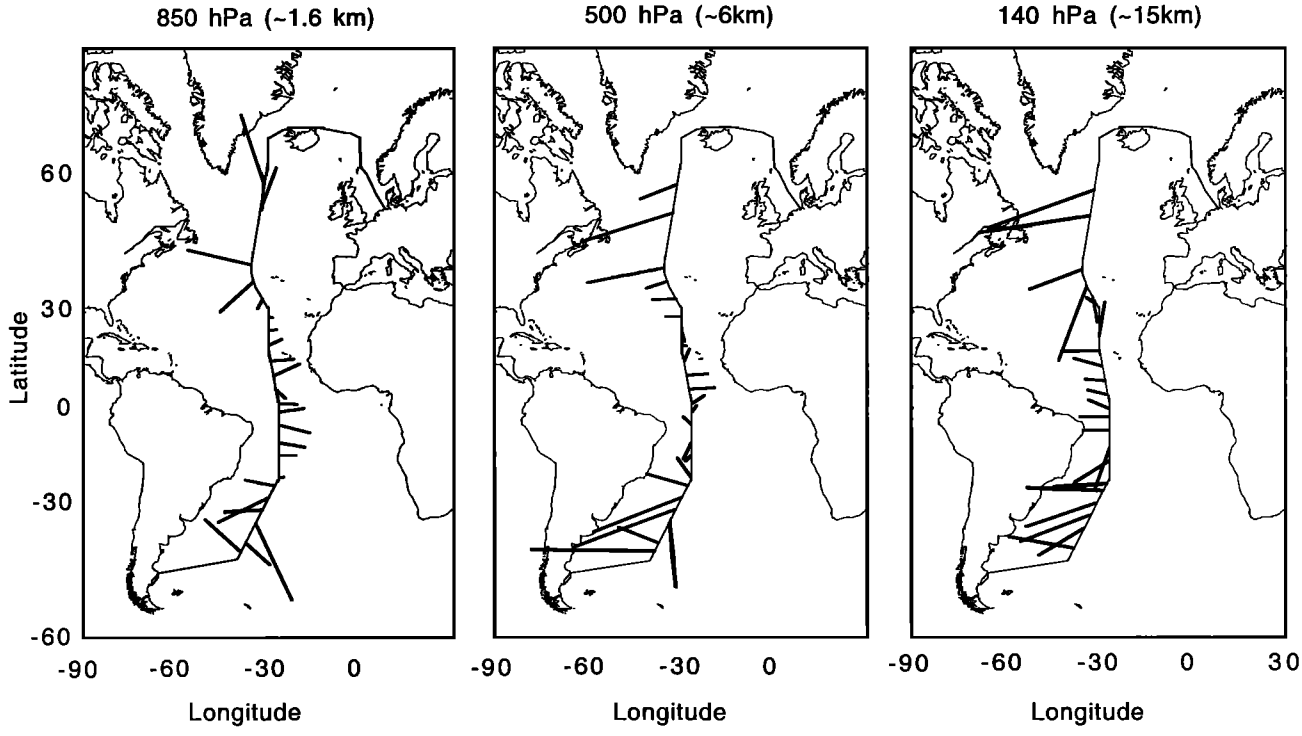

Figure 3. Backward trajectories for three pressure levels. The 850 hPa trajectories (~1.6 km) have been calculated for 48 hours, the ones at 500 hPa (~6 km) for 36 hours, and the ones at 140 hPa (~15 km) for 24 hours. For clarity, only the starting and ending points of the trajectories are plotted.

The differences in the results of both analysis methods are much higher for the partial columns (20%) than for the total columns (5%). This is because the partial columns are much more sensitive to differences in the retrieval methods and, overall, the compensating effects of the different altitude layers reduced the variabilities in the total columns.

5. Results

5.1. Characteristics of the Cruise Observations

For interpretation of the shorter-lived trace gases, the origin of the air masses probed must be considered. Figure 3 shows backward trajectories for three levels calculated by the German Weather Forecast. For the lowest level at 850 hPa (~1.6 km) the 48-hour back trajectories are given. The back trajectories for the 500 hPa level (~5.0 km) are calculated for a 36-hour period. For the level at 140 hPa (~15 km), only 24-hour back trajectories were available. For clarity, only the starting and ending points of the trajectories are plotted. At 850 hPa in the tropics the winds are coming from Africa (trade winds), while the trajectories at 140 hPa indicate air masses originating from South America (anti trade winds). Furthermore, for tropospheric trace gases the position of the ITCZ (Intertropical Convergence Zone) must be considered. The ITCZ, located at 7°–8°N in October 1996 in the Atlantic, visible in the 850 hPa trajectories by the converging trade wings, represents an efficient tropospheric border between the air masses from both hemispheres.

It is important to note that our observations were performed during the season of intense biomass burning. Biomass burning, such as the natural burning of grassland or deforestation, leads to high levels for several tropospheric trace gases, especially in the tropics [*Andreae et al.*, 1996; *Levine*, 1996]. The maximum intensity is typically found during October–November [*Granier et al.*, 1996].

The total column densities for all trace gases are given in Table 3, averaged for latitudinal steps of 5°. In addition to the total columns, the table gives average mixing ratios for the tropospheric trace gases for the altitude range 0–12 km, as derived from the scaled vmr profiles. Furthermore, for C_2H_6, CH_2O, and COS appropriate in situ data are given for comparison. For most trace gases the total columns are plotted in Figure 4a–4g. Furthermore, the tropopause altitudes, as derived from the balloon sondes, are plotted in Figure 4h.

5.2. Long-Lived Tropospheric Trace Gases

N_2O and CH_4 both have a long lifetime in the troposphere and relatively constant mixing ratios. The latitudinal decrease in their total columns (Table 3) is mainly caused by the poleward decrease of the tropopause altitude (compare with the tropopause altitude in Figure 4h) and stratospheric descent. Since both trace gases decrease in their mixing ratio above the tropopause, the ratio CH_4/N_2O (Figure 4a) depends mainly on interhemispheric differences in their mixing ratios, and only to a minor extent on variations in the tropopause height and stratospheric descent. The measured ratio is about 3% higher in the north compared to the south. The gradient in the ratio occurs at about 10°N, in agreement with the position of the ITCZ. Since N_2O does not show an interhemispheric difference, the difference in the ratio can be attributed to the interhemispheric difference in CH_4. According to the WMO assessment [*WMO*, 1995], atmospheric CH_4 concentrations in the Southern

Table 3. Total Column Densities for All Trace Gases Together With the Averaged Mixing Ratios for the Altitude Region 0–12 km.

	Latitude, deg																		
	60–55N	50–45N	45–40N	40–35N	35–30N	30–25N	25–20N	20–15N	15–10N	10–5N	5–0N	0–5S	5–10S	10–15S	15–20S	20–25S	25–30S	30–35S	40–45S
HCN																			
x10^{15}	...	...	...	...	...	4.81	2.79	3.19	3.68	4.18	4.08	4.14	4.53	5.03	4.59	4.18	3.86	...	...
pptv	...	...	...	...	...	220	109	138	182	198	190	186	196	223	200	159	172	...	...
C_2H_2																			
x10^{15}	...	...	...	...	...	0.59	0.48	...	0.51	1.41	1.86	2.00	1.39	1.88	2.30	...	1.39	...	...
pptv	...	...	...	...	...	29	18	...	22	76	101	110	73	101	134	...	77	...	...
C_2H_6																			
x10^{16}	1.91	1.64	0.82	0.74	1.09	1.07	0.96	0.88	0.82	0.82	0.71	0.96	0.92	1.07	1.13	0.96	0.71	0.78	0.46
pptv	1067	892	390	339	528	561	496	438	399	397	303	452	467	531	555	431	366	406	245
In situ*	1050	1000	531	486	674	757	574	580	478	467	350	340	361	318	330	319	351	340	367
CO																			
x10^{18}	1.89	2.12	1.52	1.58	1.61	1.64	1.57	1.64	1.70	1.85	1.87	2.03	1.87	1.97	1.98	...	1.44	1.37	...
ppbv	103	115	80.1	82.9	85.2	86.6	82.1	85.4	89.2	96.0	96.7	104	100	101	97.1	...	76.3	75.1	...
O_3																			
x10^{18}	7.76	7.62	6.96	7.32	7.11	7.31	7.20	7.04	...	6.76	6.81	6.59	7.37	6.87	7.34	6.90	7.29	...	...
ppbv	71	51	34	34	37	37	38	36	...	31	32	31	53	38	40	44	42	...	...
COS																			
x10^{16}	0.95	1.04	1.09	1.05	1.03	1.06	1.09	1.13	1.05	1.09	1.09	1.07	1.08	1.08	1.05	...	1.11	1.07	...
pptv	467	494	537	499	492	506	512	536	490	513	510	504	511	510	499	...	535	516	...
In situ*	...	436	458	418	464	452	444	474	500	501	509	485	475	461	447	450	461	...	...
CH_4																			
x10^{19}	3.60	3.64	3.55	3.59	3.60	3.63	3.65	3.63	3.62	3.58	3.55	3.60	3.61	3.60	3.59	3.53	3.52	3.50	...
ppmv	1.78	1.76	1.71	1.71	1.71	1.72	1.72	1.71	1.72	1.69	1.67	1.70	1.70	1.70	1.70	1.68	1.69	1.70	...
N_2O																			
x10^{18}	6.27	6.38	6.32	6.40	6.44	6.47	6.55	6.52	6.47	6.51	6.50	6.57	6.55	6.58	6.56	6.44	6.48	6.40	...
ppbv	310	304	303	305	306	307	309	307	304	307	306	310	309	311	311	308	312	309	...
CFC–12 (CF_2Cl_2)																			
x10^{16}	1.02	1.08	1.06	1.05	1.07	1.07	1.08	1.07	...	1.06	1.06	1.04	1.07	1.07	1.07	1.06	1.04	1.04	...
pptv	509	519	525	505	516	516	513	511	...	505	501	494	509	507	513	511	506	504	...
CFC–22 (CHF_2Cl)																			
x10^{16}	2.53	2.44	2.60	3.10	2.98	2.45	2.66	2.01	...	2.52	2.55	2.71	1.99	1.98	2.37	2.17	2.50	...	...
pptv	122	114	125	147	140	115	124	94.0	...	118	119	127	93.6	92.7	112	103	118	...	...
CH_2O																			
x10^{16}	0.55	0.39	0.95	0.97	1.49	1.01	1.46	0.64	0.67	1.31	1.31	1.43	1.23	1.19	0.85	1.72	0.87	3.82	3.54
pptv	315	223	545	574	863	582	845	369	383	756	756	826	710	688	487	996	501	217	200
In situ*	...	202	298	401	637	518	575	932	487	998	985	783	715	369	797	112	505	340	...
H_2O																			
x10^{23}	0.38	0.39	1.56	1.57	1.31	0.95	1.15	1.27	1.41	1.85	1.59	1.43	1.03	0.80	0.77	1.24	0.66	0.77	0.54
ppmv (x100)	22	23	91	92	77	55	67	74	83	108	93	84	60	47	45	72	39	45	31

Note that no FTIR spectrometer values exist for the latitude regions 55°–50°N and 35°–40°S.

*In addition to the mixing ratios derived from the FTIR observations data of in situ observations are given. C_2H_6, CH_2O: Measured on board the *Polarstern* during the cruise. COS: Measured in October–November 1997 on the central Atlantic (Xiaobin Xu, personal communications, 1999).

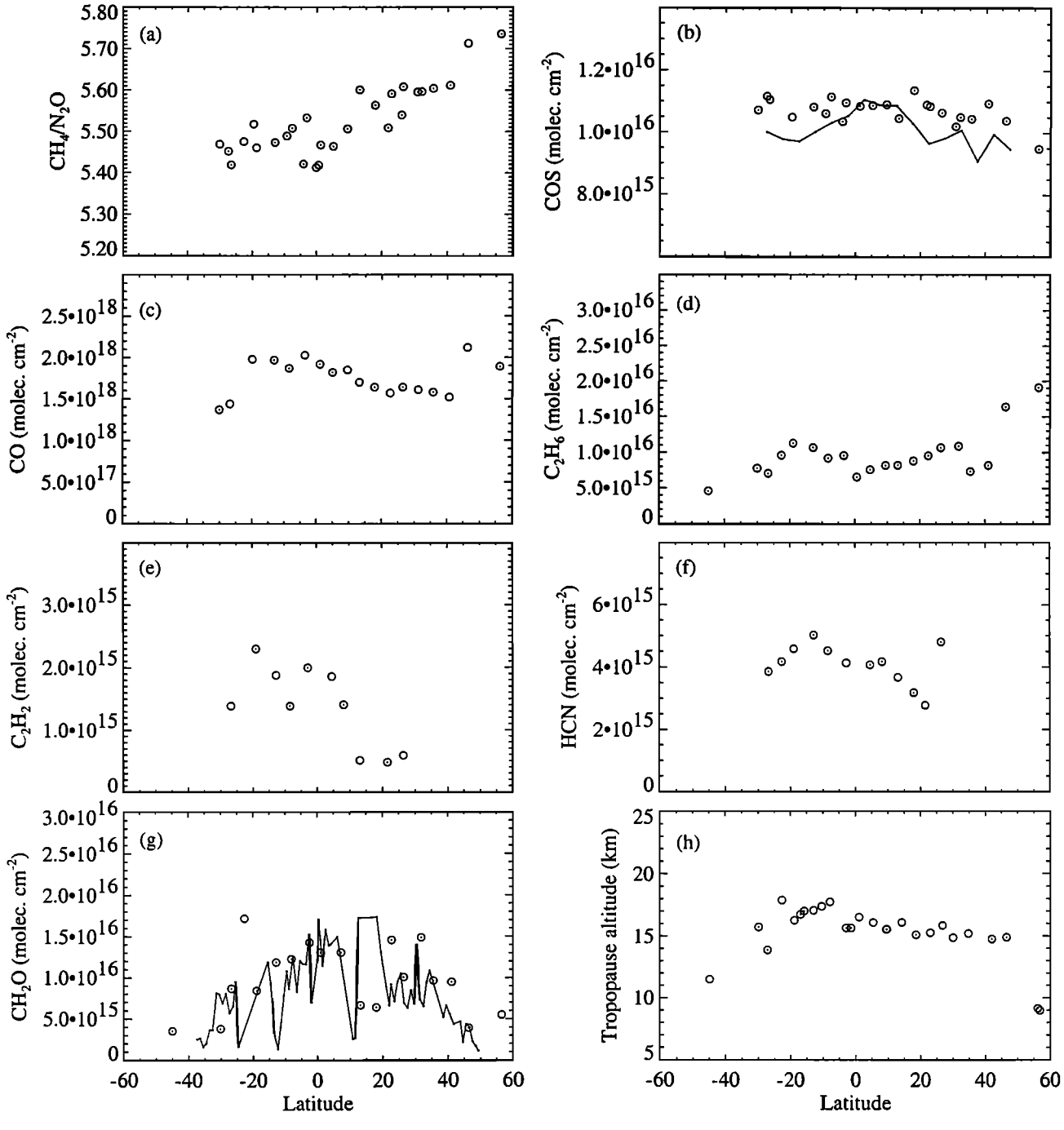

Figure 4. Total column densities of several trace gases measured spectroscopically during the cruise (circles) together with in situ data for CH2O and COS (lines), converted to total columns as explained in the text, and the tropopause altitude.

Hemisphere are on the average about 6% lower than in the Northern Hemisphere. The difference in our observations is most likely caused by the seasonal variability of CH_4.

Total columns of COS are given in Table 3 and Figure 4b. Mixing ratios have been calculated from the FTIR observations using the scaled vmr profiles. For comparison, in situ data, measured during a cruise in October–November 1997 on the Atlantic (Table 3, X. Xu and H. Bingemer, unpublished results, 1999) have been given. The agreement of the in situ data with the FTIR ones indicates that COS is uniformly distributed throughout the tropopause.

To further facilitate comparision with our total column results in Figure 4b, the in situ data have been converted to total columns. COS columns (line in Figure 4b) have been calculated assuming that the mixing ratios at all altitudes equal the in situ values from the ground. The agreement of the total numbers calculated in this way with our measured FTIR data suggests that the COS vmr profile is constant throughout the troposphere

and lower stratosphere, where total column observations of tropospheric trace gases are most sensitive. Above about 20 km the decrease in the molecule number density with altitude limits the sensitivity of the COS total column measurements. A constant mixing ratio of COS at least up to 20 km is in agreement with the observation that the latitudinal variation in the tropopause altitude (Figure 4h) does not show up in the FTIR total column measurements of COS.

Our cruise data, together with the in situ data, do not show any interhemispheric variability. On the contrary, by using ground-based FTIR data from a few stations, *Griffith et al.* [1998] observed a north/south interhemispheric ratio of 1.1–1.2. Also, previous in situ measurements on the central Atlantic give a northward increase of COS, which was tentatively interpretated as evidence for COS contributions by anthropogenic sources [*Bingemer et al.*, 1990].

5.3. Shorter-Lived Trace Gases

5.3.1. Total column results. The total columns for a few shorter-lived tropospheric trace gases are given in Figures 4c–4g. For comparison with other ground-based total column measurements, the secular trend must be considered (CO, C_2H_6 and CH_2O: < 1%/y; C_2H_2 and HCN: < 0.5%/y [*WMO*, 1995; *Notholt et al.*, 1997b]). CO and C_2H_6 (Figures 4c, and 4d) show maxima in their total columns north of 40°N and in the tropics. Both trace gases have similar anthropogenic sources at the ground [*Smyth et al.*, 1996]. In addition, CO is produced by the photooxidation of CH_4 and nonmethane hydrocarbons (NMHCs). In situ measurements of several NMHCs on board the *Polarstern* during the cruise do not indicate any substantial increase within the tropics (R. Koppmann, personal communications, 1999). Assuming a weak altitude gradient of the NMHCs throughout the troposphere, as measured by *Talbot et al.* [1996] during the TRACE A campaign in September–October 1992 above the Atlantic, the in situ data of the NMHCs allow us to exclude the formation of CO by the oxidation of the NMHCs.

The lifetimes of both trace gases within the tropics and subtropics are longer than typical meridional transport times but shorter than zonal transport times [*Attkinson*, 1990; *Smyth et al.*, 1996]. Thus processes at different longitudes are more likely to influence our observations than processes at different latitudes. Observations throughout the TRACE A campaign and sattelite data suggest an impact of biomass burning on the trace gas concentrations on the tropical south Atlantic [*Andreae et al.*, 1996; *Levine*, 1996; *Talbot et al.*, 1996]. The substantial increase north of 40°N can most likely be attributed to the anthropogenic combustion, and the high values in the tropics are probably caused by biomass burning emissions.

Infrared spectroscopic observations were performed between 1970 and 1985 by *Dianov-Klokov and Yurganov* [1989] and *Dianov-Klokov et al.* [1989] during several ship cruises on the Atlantic and at a few measurement stations on land. The observations were recorded with a low-resolution grating spectrometer. They deduced a long-term increase of 1.5–2% in the Northern Hemisphere and about 0.6% in the Southern Hemisphere. For the period 1970–1985 they obtained average total columns of 2.0×10^{18} molecules cm^{-2} north of 40°N, a weak maximum of about 2.2×10^{18} molecules cm^{-2} in the tropics, and minimum values of 1.1×10^{18} molecules cm^{-2} at 30°S for comparable autumn periods. Thus their total columns measured between 1970 and 1985 agree with our observations from 1996 (Table 3) and do not indicate any significant long-term CO trend. However, as mentioned by *Dianov-Klokov and Yurganov* [1989] and *Dianov-Klokov et al.* [1989], any long-term trend for CO is difficult to quantify due to the strong seasonal and spatial variability of this species.

The results of CO and C_2H_6 have been compared with similar FTIR total column ground-based measurements performed since 1992 year-round in the Arctic at 79°N, 12°E [*Notholt et al.*, 1997a] and in the Antarctic at 78°S, 167°S [*Notholt et al.*, 1997b] in September–October 1986. The cruise data north of 40°N agree with the Arctic observations during October–November (2.0×10^{18} molecules cm^{-2} for CO and 1.8×10^{16} molecules cm^{-2} for C_2H_6, [*Notholt et al.*, 1997a]), indicating a uniform distribution of both trace gases in the remote Northern Hemisphere. The Antarctic observations from September–October 1986 of 0.9×10^{18} molecules cm^{-2} for CO [*Notholt et al.*, 1997b] are lower than our cruise data at southern latitudes, suggesting a further concentration gradient of CO between southern mid-latitudes and the pole. For C_2H_6 the total columns of 0.6×10^{16} molecules cm^{-2} measured in the Antarctic [*Notholt et al.*, 1997b] agree with our cruise data at southern latitudes.

The total columns of C_2H_2 are illustrated in Figure 4e. Due to its spectral interference by strong water lines, C_2H_2 is much more difficult to detect than CO or C_2H_6. Our data give high values in the tropics. North of 10°N, the total columns are close to the detection limit. In situ data of C_2H_2, measured during the cruise (R. Koppman, preliminary results, 1999) reveal a similar latitudinal variability. This compound has sources that are similar to those of CO or C_2H_6, but the C_2H_2 lifetime is only a few days under sunlight [*Attkinson*, 1990]. Thus the zonal transport times from the continents on the middle of the Atlantic are of the same order as the atmospheric lifetime of this species. Therefore the total columns measured on board the *Polarstern* can most likely be attributed to combustion processes on the surrounding continents, in agreement with observations by *Talbot et al.* [1996].

Although only a few data points exist, it is evident that the latitudinal variability of C_2H_2 is much more pronounced than that of CO or C_2H_6, probably caused by the much shorter lifetime of this species. This assumption is consistent with our measurements from the Arctic [*Notholt et al.*, 1997a], where the seasonal cycle of C_2H_2 is found to be 3 times more pronounced than for CO and C_2H_6. The cruise data are 2–6 times lower than our observations in Spitsbergen during October–November (4×10^{15} molecules cm^{-2} [*Notholt et al.*, 1997a]), indicating a well-pronounced gradient toward the north. In the Southern Hemisphere the C_2H_2 cruise columns are slightly higher than in Antarctica (0.8×10^{15} molecules cm^{-2} [*Notholt et al.*, 1997b]), probably because other than tropical biomass burning, no strong emissions exist.

Figure 4f presents measured total columns of HCN. This compound is difficult to detect in situ, and so remote observations in the infrared are one of the few measurement techniques [*Coffey et al.*, 1981]. HCN is produced at the ground by agriculture, biomass burning, and production of coke. Its main loss pathway is its reaction with OH. The estimated lifetime of HCN is of the order of 1–5 years [*Mahieu et al.*, 1997]. The latitudinal variation of this trace gas in the troposphere has not been measured thus far. Our data show a clear maximum in the tropics of the Southern Hemisphere. Unfortunately, no spectra in the region where HCN absorbs have been recorded north of 30°N, which could confirm the measured increase in the north. *Mahieu et al.* [1997] derived a mixing

ratio of 180 pptv for background conditions from IR spectra recorded at the Jungfraujoch. Our mixing ratios derived (Table 3) are slightly higher, consistent with the proximity of biogenic sources at that latitude. The maximum total columns observed in the tropics are comparable to our October observations from the Arctic (4–5x10^{15} molecules cm^{-2} [*Notholt et al.*, 1997a]) but higher than our data from the Antarctic (2.6x10^{15} molecules cm^{-2} [*Notholt et al.*, 1997b]).

The observed total columns of CH_2O (Figure 4g) show a clear maximum in the tropics. The compound is emitted at the ground or produced by the oxidation of methane or NMHCs. The short lifetime of only a few hours under sunlight [*Attkinson*, 1990] allows us to exclude direct emissions from the continents as a source for our high columns measured. In situ measurements of several NMHC's during the cruise do not indicate any substantial increase within the tropics (R. Koppmann, personal communications, 1999). Assuming a weak altitude gradient of the NMHC's throughout the troposphere [see *Talbot et al.*, 1996], the formation via NMHCs can also be excluded. We therefore attribute the high total columns of CH_2O to the formation via methane oxidation. Since this process depends on the sunlight intensity, a maximum in the tropics can be expected, in agreement with these cruise observations. Our total column data in the tropics are much higher than our Arctic results of 2x10^{15} molecules cm^{-2} [*Notholt et al.*, 1997a] and our Antarctic data of 0.8x10^{15} molecules cm^{-2} [*Notholt et al.*, 1997b], underlining the importance of the methane oxidation as a source of CH_2O.

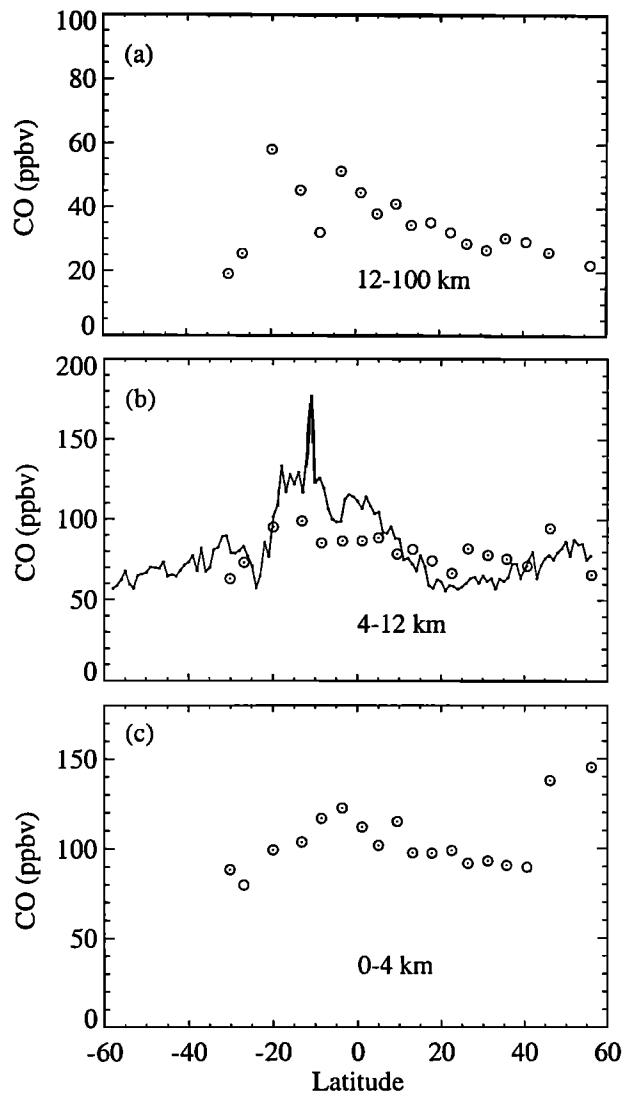

Figure 5. Mixing ratios for CO for three altitude layers as retrieved from the Fourier transform infrared (FTIR) spectra. The CO data from the Measurement of Air Pollution From Satellites (MAPS) satellite experiment for October 1994 at around 30°E [see *Conners et al.*, 1996] are plotted in Figure 5b as a line.

Table 4. Area of Deforestation in South America as Obtained by Satellite Observations

Deforestation, Period	Area, km^2
1978–1988	21130
1988–1989	17860
1989–1990	13810
1990–1991	11130
1991–1992	13786
1992–1994	14896
1994–1995	29059
1995–1996	18161
1996–1997	13227

P. Artaxo, personal communications, 1998; see also www.inpe.br/Informacoes_Eventos/amz/amz.html

In addition to our FTIR measurements, CH_2O was also measured on board the *Polarstern* by in situ techniques. The in situ data are given in Table 3. To facilitate comparision with our total column data, the in situ ones have been converted to total columns. These columns have been calculated assuming the mixing ratios to equal the in situ data up to a specified altitude, the "layer thickness". Above that altitude the mixing ratios are set to be zero. For a layer thickness of 9 km the columns so calculated agree with our measured FTIR data (Figure 4g). The agreement of both curves at all latitudes assuming a constant layer thickness indicates that the shape of CH_2O vmr profile does not show a strong latitudinal variability. Furthermore, the use of a layer thickness of 9 km indicates that the concentrations of this compound are relatively high in the whole troposphere.

5.3.2. Concentration profiles of CO, C_2H_6, and O_3. In order to investigate the composition of the free troposphere in more detail, the mixing ratios for CO, C_2H_6, and O_3 have been determined for a few atmospheric layers. The CO mixing ratios retrieved from the FTIR spectra for the layer 0–4 km (Figure 5c) reveal a weak maximum in the tropics and a substantial increase north of 40°N.

Figure 5b gives the partial columns retrieved for the altitude layer 4–12 km. In addition, CO data measured by the Measurement of Air Pollution From Satellite (MAPS) instrument in October 1994 at around 30°E onboard the space shuttle [see *Conners et al.*, 1996] have been included in Figure 5b. For a comparision the sensitivities of both instruments must be considered. The averaging kernels of the satellite instrument peak at 300 mbar and decrease in the lower troposphere [*Pougatchev et al.*, 1998]. Therefore the satellite instrument yields midtropospheric average mixing ratios, comparable to the results of our profile retrieval for the altitude region 4–12 km (see Figure 2).

The MAPS data of October 1994 in the tropics are higher by 30% than our cruise data for the same period, which we attribute mainly to the variability in the tropical biomass burning. As measured by the MAPS satellite, the highest CO concentrations on the tropical Atlantic are reported in October–November, the

season of the most intense biomass burning [*Andreae et al.*, 1996; *Levine*, 1996]. Furthermore, observations throughout the TRACE A campaign suggest an impact of biomass burning on the trace gas concentrations in the tropical south Atlantic [*Talbot et al.*, 1996]. A suitable indicator of the variability of the tropical biomass burning is given by the area of deforestation, as calculated from fire statistics measured by satellite [e.g., *Thompson et al.*, 1996]. Table 4 gives the area of deforestation in South America as obtained by satellite observations (P. Artaxo, personal communications, 1998; see also www.inpe.br/Informacoes_Eventos/amz/amz.html). The data show that in 1994–1995 the deforested area was nearly double the area in 1996–1997, in agreement with the CO data in Figure 5b. The layer above 12 km (Figure 5a) reveals a maximum in the tropics of the Southern Hemisphere, in contrast to the bottom layer.

For C_2H_6 (Figure 6) the spectral line shape allows us to retrieve the partial columns only in one tropospheric layer, 0–12 km (see Figure 2). The retrieval yields a similar latitudinal variation of the mixing ratio as for CO: high values north of 40°N below 12 km and a concentration maximum in the tropics for the altitudes above 12 km.

The FTIR data of CO and C_2H_6 for the bottom layer have been compared with in situ observations performed during the cruise variation (R. Koppmann, preliminary results, 1999). For C_2H_6 the in situ data are plotted in Figure 6b. In the tropics of the Southern Hemisphere the total columns of both compounds are about 30–50% higher than the in situ observations. One possible explanation might be that in this part of the troposphere the average mixing ratios are higher than directly at the surface, where the in situ data have been taken. This result would be consistent with the observation that the highest concentrations

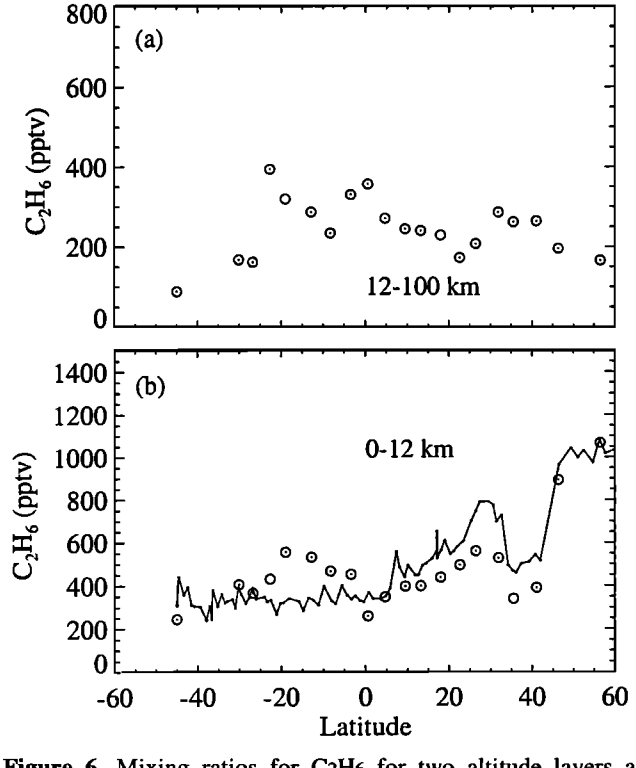

Figure 6. Mixing ratios for C2H6 for two altitude layers as retrieved from the FTIR spectra (circles) together with in situ data measured at sea level (line).

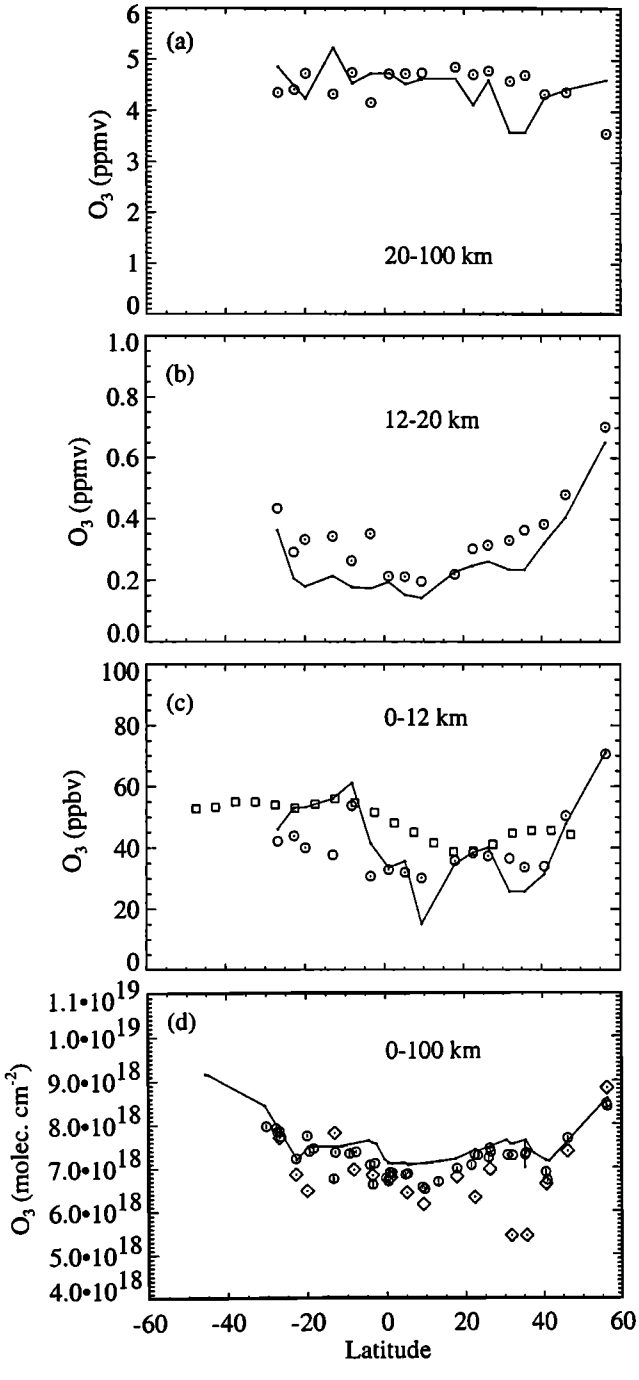

Figure 7(a–c). Mixing ratios for O3 for three altitude layers as retrieved from the FTIR spectra (circles) together with the results from the Electrochemical Cell (ECC) balloons (line) and tropospheric residual climatology data (squares). (d) Comparison of the total columns derived by the FTIR (squares), the balloon (circles), Total Ozone Mapping Spectrometer (TOMS) satellite (line).

of several pollutants, including CO and C_2H_6, are found not directly at the surface but at higher altitudes [*Talbot et al.*, 1996] because in the free troposphere the colder temperatures and lower OH concentrations increase the lifetimes of these species. However, it must be considered that with our data sets we cannot exclude systematic differences between the in situ data and our FTIR results, which would yield wrong conclusions.

In the interpretation of the results for CO, the contribution by methane oxidation has to be considered, especially for the higher altitudes, where no direct emissions exist. However, since C_2H_6 has its main source at the ground and due to the similarity of the latitudinal variations of CO and C_2H_6 above 12 km, the mixing ratios for CO above 12 km are assumed to be mainly caused by emissions at the ground, followed by an efficient convective uplift and horizontal transport. Thus compared to the impact by emissions, the contribution from methane oxidation can be neglected above approximately 12 km.

For O_3 (Figures 7a–7d) the spectral line shape allows us to retrieve the partial columns in only one tropospheric layer, 0–12 km (see Figure 2). The results have been compared with in situ data from sondes (Figures 7a–7d) and with tropospheric residual climatology data (Figure 7c), based on Stratospheric Aerosol and Gas Experiment (SAGE) 1 and 2 and Total Ozone Mapping Spectrometer (TOMS) V6.0 and V7.0 total ozone data for September to November [e.g., *Fishman et al.*, 1996]. All three data sets show reasonable agreement. North of 40°N a strong increase in the mixing ratios can be observed for the layers 0–12 km and 12–20 km. In the tropics of the Southern Hemisphere the sondes and the satellite data give enhanced values which are confirmed by the FTIR data on only one occasion. Furthermore, the total columns for O_3 have been compared with the results of the Electrochemical Cell (ECC) ozone balloon sondes and the TOMS satellite data (Figure 7d). Except for two balloon launches at 30°–36°N and slightly higher TOMS data around 10°N all three data sets agree to within 5% and do not indicate any systematic differences.

The ozone concentrations measured in the tropical troposphere of the Southern Hemisphere agree with observations by *Thompson et al.* [1996], who measured high O_3 concentrations in the free tropical troposphere during the 1992 TRACE A and Southern African Fire–Atmosphere Research Inititiative (SAFARI) campaigns and attributed them to the tropical biomass burning. Therefore the high ozone concentrations measured during the cruise may be the result of photochemical processes, in agreement with our high concentrations of CO and C_2H_6 measured there. The increase north of 40°N for the altitude layer 0–12 km cannot be assigned to elevated ozone concentrations in the troposphere. Owing to the decrease in the tropopause altitude, a portion of the high mixing ratios is probably caused by stratospheric ozone, as can be seen by comparing the results with the data for the layer 12–20 km.

The cruise data for the upper altitude levels above 12 km can be compared with ATMOS/ATLAS satellite observations from November 1994 [*Rinsland et al.*, 1998b], which covered the upper troposphere above the minimum tangent altitude of typically 11 km. The satellite observations of CO, C_2H_6, C_2H_2, and HCN yielded enhanced mixing ratios in the tropics (5°N to 31°N), which were attributed to biomass burning emissions.

6. Conclusions

The cruise observations have allowed the retrieval of the latitudinal variations of the total column densities of several important trace gases, even in the tropics under high humidities. In addition, for a few trace gases the vertical distributions were retrieved. The comparison with in situ values emphasizes the feasibility of profile retrieval using high-spectral-resolution ground-based FTIR spectra.

For the long-lived trace gas CH_4 the analysis gives an interhemispheric difference of 3%, in reasonable agreement with in situ observations at the ground. The shorter-lived trace gases show strong variabilities in their concentrations. North of 40°N, high total columns of CO and C_2H_6 are found. The observations in the tropics of the Southern Hemisphere yield high tropospheric concentrations of CO, C_2H_6, C_2H_2, O_3, and HCN. The peak in the total columns of CH_2O in the tropics is most probably caused by the formation via CH_4 oxidation.

The results for the profile retrieval of CO, C_2H_6, and O_3 give some insight into the transport processes of trace gases in the free troposphere. The high mixing ratios of CO and C_2H_6 northward of 40°N are confined to below 12 km. For CO the data indicate that the high mixing ratios are evenly concentrated below 4 km. This means that north of 40° pollutants emitted at the ground stay in the altitude range below 12 km during the long-range transport over the central Atlantic. In contrast, in the tropics relatively high mixing ratios of CO and C_2H_6 are also found above 12 km altitude.

This implies that trace gases emitted in the tropics are not only transported horizontally, but are uplifted by the intense tropical convection to the upper troposphere, followed by an efficient zonal transport. The high mixing ratios measured above 12 km suggest an influence of tropical tropospheric emissions on stratospheric chemistry. For example, besides other compounds, biomass burning leads to elevated concentrations of CH_3Cl [e.g., *Levine*, 1996]. If this compound is able to enter the stratosphere, its photodissociation leads to chlorine atoms, which are directly involved in ozone catalytic destruction cycles.

Since most tropospheric trace gases are destroyed by reaction with OH, our data set together with an appropriate model, would provide important constraints on estimates of the oxidation capacity in the free troposphere [e.g., *Granier et al.*, 1996]. Because ground-based FTIR spectroscopy allows simultaneous monitoring of several tropospheric trace gases, having the same sources but different lifetimes, the oxidation capacity could be determined independent of variabilities in the sources. Profile retrievals of the compounds might allow an estimate of the vertical concentration profile of OH. The oxidation capacity is expected to change on a long-term basis, due to the increase in UV radiation, which is attributed to the decrease of stratospheric ozone [*Houghton et al.*, 1996]. Ship-borne column measurements on a regular basis could be important in the monitoring of the latitudinal dependence of long-term changes in the oxidation capacity of the free troposphere.

Acknowledgments. We gratefully acknowledge V. S. Conners (NASA Langley) for the MAPS CO data, P. Artaxo (NASA Langley) for unpublished data on the fire statistics, R. McPeters (NASA Goddard Space Center) for the TOMS satellite data, J. Fishman and A. Balok (NASA Langley) for SAGE tropospheric residual O_3 data, Xiaobu Xu and H. Bingemer (Institute for Meterology and Geophysics, University of Frankfurt) for in situ data on COS, and T. Brauers and R. Koppmann (FZJ, Jülich) for unpublished CO and NMHC concentrations, measured during the campaign. Furthermore, we acknowledge P. Kaufeld and R. Strüfing from the German Weather Forecast for the calculation of the backward trajectories. We thank L. Chiou of Science Applications International Corporation for her help in the analysis of the cruise spectra at NASA Langley and the preparation of several figures. M. Archer of Professional English, Newport News, Virginia, helped edit the manuscript. A. Keens and J. Gast (Bruker GmbH) are acknowledged for technical support. The work was partly funded by the DFG within contract 447 NSL-

111/1/98. Research at NASA Langley Research Center was funded by NASA's Upper Atmosphere Research Program and NASA's Atmospheric Chemistry Modeling and Analysis Program. Contribution 1638 of the Alfred Wegener Institute.

References

Andreae, M. O., J. Fishman, and J. Lindesay, The Southern Tropical Atlantic Region Experiment (STARE): Transport and Atmospheric Chemistry near the Equator–Atlantic (TRACE A) and Southern African Fire–Atmosphere Research Initiative (SAFARI): An introduction, *J. Geophys. Res.*, *101*, 23,519–23,520, 1996.

Angeletti, G., and G. Restelli (Eds., Physico–Chemical Behaviour of Atmospheric Pollutants, Proceedings of 6th European Symposium, Varese, 18–22 October 1993, *Eur. Comm. Rep. EUR 15609/1–2 EN*, Eur. Comm. Brussels,1994.

Attkinson, R., Gas–phase tropospheric chemistry of organic compounds: A review, *Atmos. Environ., 24A*, 1–41, 1990.

Bingemer, H. G., S. Bürgermeister, and R. L. Zimmermann, H.–W. Georgii, Atmospheric OCS: Evidence for a contribution of anthropogenic sources?, *J. Geophys. Res.*, *95*, 20,617–20,622, 1990.

Brown, L. R., M. R. Gunson, R. A. Toth, F. W. Irion, C. P. Rinsland, and A. Goldman, The 1995 Atmospheric Trace Molecule Spectroscopy (ATMOS) linelist, *Appl. Opt., 35*, 2828–2848, 1996.

Coffey, M.T., W.G. Mankin, and R.J. Cicerone, Spectroscopic Detection of Stratospheric Hydrogen Cyanide, *Science, 214*, 333–335, 1981.

Conners, V. S., M. Flood, T. Jones, B. Gormsen, S. Nolf, and H. G. Reichle Jr, Global distribution of biomass burning and carbon monoxide in the middle troposphere during early April and October 1994, in *Biomass Burning and Global Change*, edited by J. Levine, pp. 99–106, MIT Press, Cambridge, Mass., 1996

Connor, B. J., A. Parrish, J.–J. Tsou, and M. P. McCormick, Error analysis for the ground–based microwave ozone measurements during STOIC, *J. Geophys. Res., 100*, 9283–9291, 1995.

Dianov–Klokov, V. I., and L. N. Yurganov, Spectroscopic measurements of atmospheric carbon monoxide and methane, 2, Seasonal variations and long–term trends, *J. Atmos. Chem., 8*, 153–164, 1989.

Dianov–Klokov, V. I., L. N. Yurganov, E. I. Grechko, and A. V. Dzhola, Spectroscopic measurements of atmospheric carbon monoxide and methane, 1, Latitudinal distribution, *J. Atmos. Chem., 8*, 139–151, 1989.

Fishman, J., V. G. Bracket, E. V. Browell, and W. B. Grant, Tropospheric ozone derived from TOMS/SBUV measurements during TRACE A, *J. Geophys. Res.*, *101*, 24,069–24,082, 1996.

Graedel, T. E., and P. J Crutzen, *Atmospheric Change: An Earth System Perspective*, W. H. Freeman, New York, 1993.

Granier, C., W. M. Hao, G. Brasseur, and J.–F. Müller, Land–use practices and biomass burning: Impact on the chemical composition of the atmosphere, in: *Biomass Burning and Global Change*, edited by J. Levine, pp. 140–148, MIT Press, Cambridge, Mass., 1996.

Griffith, D. W. T., N. B. Jones, and W. A. Matthews, Interhemispheric ratio and annual cycle of carbonyl sulfide (OCS) total column from the ground–based solar Fourier transform infrared spectra, *J. Geophys. Res.*, *103*, 8447–8454, 1998.

Gunson, M. R., et al., The Atmospheric Trace Molecule Spectroscopy Experiment: Deployment on the Atlas space shuttle missions, *Geophys. Res. Lett., 23*, 2333–2336, 1996.

Hoell, J. M., D. D. Davis, S. C. Liu, R. Newell, M. Shipham, H. Akimoto, R. J. McNeal, R. J. Bendura, and J. W. Drewry, Pacific Exploratory Mission–West A (PEM–West A): September–October 1991, *J. Geophys. Res.*, *101*, 1641–1653, 1996.

Hoell, J. M., D. D. Davis, S. C. Liu, R. Newell, H. Akimoto, R. J. McNeal, and R. J. Bendura, Pacific Exploratory Mission–West Phase B: February–March 1994, *J. Geophys. Res.*, *102*, 28223–28239, 1997.

Houghton, J. T., L. G. Meira Filho, B. A. Callander, N. Harris, A. Kattenberg, and K. Maskell (Eds.), *Climate Change 1995: The Science of Climate Change*, Cambridge Univ. Press, New York, 1996.

Jones, N. B., M. Koike, W. A. Matthews, and B. M. McNamara, Southern Hemisphere mid–latitude seasonal cycle in total column nitric acid, *Geophys. Res. Lett., 21*, 593–596, 1994.

Levine, J. S (Ed.), *Biomass Burning and Global Change*, MIT Press, Cambridge, Mass., 1996.

Mahieu, E., R. Zander, L. Delbouille, P. Demoulin, G Roland, and C. Servais, Observed trends in total vertical column abundances of atmospheric gases from IR solar spectra recorded at the Jungfraujoch, *J. Atmos. Chem., 28*, 227–243, 1997.

Murcray, F. J., A. Goldman, R. Blatherwick, A. Matthews, and N. Jones, HNO3 and HCl amounts over McMurdo during the spring of 1987, *J. Geophys. Res., 94*, 16,615–16,618, 1989.

Notholt, J., G. Toon, F. Stordal, S. Solberg, N. Schmidbauer, A. Meier, E. Becker, and B. Sen, Seasonal variations of atmospheric trace gases in the high Arctic at 79°N, *J. Geophys. Res, 102*, 12,855–12,861, 1997a.

Notholt, J., G. C. Toon, R. Lehmann, B. Sen, and J.–F. Blavier, Comparison of Arctic and Antarctic trace gas column abundances from ground–based Fourier transform infrared spectrometry, *J. Geophys. Res., 102*, 12,863–12,869, 1997b.

Peterson, D. B., and J. J. Margitan, Upper Atmospheric Research Satellite Correlative Measurement Program (UARS–CMP) balloon data atlas, *NASA Publ.*, 1995.

Pine, A. S., and S. C. Stone, Torsional tunneling and A1–A1 splittings and air broadening of the $^rQ_0$ and $^rQ_3$ subbranches of the v7 band of ethane, *J. Mol. Spectrosc., 175*, 21–30, 1996.

Pougatchev, N. S., B. J. Connor, and C. P. Rinsland, Infrared measurements of the ozone vertical distribution above Kitt Peak, *J. Geophys. Res., 100*, 16,689–16,697, 1995.

Pougatchev, N. S., et al., Ground–based infrared solar spectroscopic measurements of carbon monoxide during 1994 Measurement of Air Pollution From Space flights, *J. Geophys. Res., 103*, 19,317–19,325, 1998.

Rao, K. N., and A. Weber, (Eds.), *Spectroscopy of the Earth's Atmosphere and Interstellar Medium*, Academic, San Diego, Calif, 1992.

Rinsland, C. P., A., Goldman, F. J. Murcray, F. H. Murcray, R. D. Blatherwick, and D. G. Murcray, Infrared measurements of atmospheric gases above Mauna Loa, Hawaii, in February 1987, *J. Geophys. Res., 93*, 12,607–12,626, 1988.

Rinsland, C. P., J. S. Levine, A. Goldman, N. D. Sze, M. K. W. Ko, and D. W. Johnson, Infrared measurements of HF and HCl total column abundances above Kitt Peak, 1977–1990: Seasonal cycles, long term increases, and comparisons with model calculations, *J. Geophys. Res., 96*, 15,523–15,540, 1991.

Rinsland, C. P., N. B. Jones, B. J. Connor, J. Logan, N. S. Pougatchev, A. Goldman, F. J. Murcray, T. M. Stephen, A. S. Pine, R. Zander, E. Mahieu, and P. Demoulin, Northern and Southern Hemisphere ground–based infrared spectroscopic measurements of tropospheric carbon monoxide and ethane, *J. Geophys. Res., 103*, 28,197–28,218, 1998a.

Rinsland, C. P., et al , ATMOS/ATLAS 3 infrared profile measurements of trace gases in the November 1994 tropical and subtropical upper troposphere, *J. Quant. Spectrosc. Radiat Transfer, 60*, 891–902, 1998b.

Rodgers, C. D., Retrieval of atmospheric temperature and composition from remote measurements of thermal radiation, *Rev. Geophys., 14*, 609–624, 1976

Rodgers, C. D. , Characterization and error analysis of profiles retrieved from remote sounding measurements, *J. Geophys. Res., 95*, 5587–5595, 1990.

Rothman, L.S., et al., The HITRAN molecular spectroscopic database and HAWKS (HITRAN atmospheric workstation): 1996 edition, *J. Quant. Spectrosc. Radiat Transfer, 60*, 665–710, 1998.

Russell, J. M., L. L. Gordley, J. H Park, S. R. Drayson, W. D. Hesketh, R. J. Cicerone, A. F. Tuck, J. E. Frederick, J. E. Harries, and P. J. Crutzen, The Halogen Occultation Experiment, *J. Geophys. Res., 98*, 10,777–10,797, 1993.

Smyth, S., et al., Comparison of free tropospheric western Pacific air mass classification schemes for the PEM–West A experiment, *J. Geophys Res., 101*, 1743–1762, 1996.

Talbot, R. W., et al., Chemical characteristics of continental outflow over the tropical South Atlantic Ocean from Brazil and Africa, *J. Geophys. Res., 101*, 24,187–24202, 1996.

Thompson, A. M., K. E. Pickering, D. P. McNamara, M. R Schoeberl, R. D. Hudson, J. H. Kim, E. V. Browell, V W. J. H. Kirchhoff, and D. Nganga, Where did tropospheric ozone over southern Africa and the tropical Atlantic come from in October 1992? Insights from TOMS, GTE TRACE A, and SAFARI 1992, *J. Geophys. Res., 101*, 24,251–24,278, 1996.

Toon, G. C., C. B. Farmer, P. W. Schaper, L. L. Lowes, and R. H. Norton, Composition measurements of the 1989 Arctic winter stratosphere by airborne infrared solar absorption spectroscopy, *J. Geophys. Res., 97*, 7939–7961, 1992.

Toon, G. C, J.-F. Blavier, J. N. Solario, and J. T. Szeto, Airborne observations of the composition of the 1992 tropical statosphere by FTIR solar absorption spectrometry, *Geophys. Res. Lett., 20*, 2503–2506, 1993.

World Metereological Organization (WMO), Scientific Assessment of Ozone Depletion: 1994, *Rep. 37*, Geneva, Schweiz, 1995.

WMO, *WMO WDCGG Data catalog*, vol. 4, *Greenhouse Gases and Other Atmospheric Gases*, Geneva, 1997.

Zander. R., P. Demoulin, E. Mahieu, G. P. Adrian, C. P. Rinsland, and A. Goldman, ESMOS II/NDSC–IR spectral fitting algorithms· Intercomparison exercise, paper presented at Atmospheric Spectroscopy Applications Workshop 1993, Univ. of Reims Champagne, Ardenne, France, 1993.

B. J. Connor and N. B. Jones, National Institute of Water and Atmospheric Research, Lauder, Private Bag 50061, Omakau, Central Otago, New Zealand.

M. Gautrois, Institute for Atmospheric Chemistry (ICG–3), Forschungszentrum Jülich, 52425 Jülich, Germany.

J. Notholt, Alfred Wegener Institute for Polar and Marine Research, Telegraphenberg A43, 14473 Potsdam, Germany. (jnotholt@awi–potsdam.de)

N. S. Pougatchev, Christopher Newport University, Physics Department, Newport News, VA 23606.

C. P. Rinsland, Atmospheric Sciences Division, NASA Langley Research Center, M.S. 401 A, Hampton, VA 23681.

O. Schrems and R. Weller, Alfred Wegener Institute for Polar and Marine Research, Am Handelshafen, 27570 Bremerhaven, Germany.

G. C. Toon, Jet Propulsion Laboratory, California Institute of Technology, M.S 183–601, 4800 Oak Grove Drive, Pasadena, CA 91109–8099.

(Received January 26, 1999; revised July 28, 1999;
accepted September 1, 1999.)